Backwater controls on the sedimentology, kinematics and geometry of bar deposits in coastal rivers

Anjali M. Fernandes[1], Virginia B. Smith[2], Kashauna G. Mason[3]

[1]The Center for Integrative Geosciences, The University of Connecticut, 354 Mansfield Road, Unit 1045, Storrs, Connecticut 06269, U. S. A. Email: anjali.fernandes@uconn.edu

[2]Villanova University 800 Lancaster Avenue Villanova, PA, 190851603, U. S. A.

[3]Department of Geosciences, 340 N. Campus Drive, 216 Gearhart Hall, University of Arkansas, Fayetteville, AR 72701, U. S. A.

Abstract

The backwater reach of coastal rivers is associated with considerable spatial and temporal variability in water and sediment flux. Here we test the hypothesis that the spatial and temporal variability in water flux and particle sizes in transport are expressed as systematic changes in the geometry of bank-attached bars across the backwater transition. Measured transverse slopes of bank-attached bars in the Mississippi and Trinity Rivers show a systematic increase as the river transitions from normal flow to the backwater. To explain this trends, we use a simple force balance relationship, in which the transverse slope of the bars constructed through traction transport varies in proportion to the square of depth-averaged flow velocity and is inversely proportional to the square of the median particle size of the supplied sediment, in bends with similar curvature. The observed trend is therefore explained by a downstream reduction in particle sizes coupled with a downstream increase in flow velocity across the backwater transition at high discharge, during which sand fluxes are greatest.

Introduction

River deposits in the coastal backwater zone display considerable spatial heterogeneity. This is likely the result of spatial and temporal non-uniformity in influences from upstream (e.g. water discharge, sediment flux) as well as downstream (e.g. sea-level, river plume dynamics). Constraining the fundamental controls on the complex geometries of sedimentary strata built by coastal rivers is essential for: (a) reconstructing Earth's past environments from shelf margin deposits, (b) characterizing reservoir properties

in shallow or deep subsurface environments, where channel deposits are the primary pathways for transport of fluids and contaminants (Kolker et al., 2013; Sawyer et al., 2015; Martin et al., 2018), and (c) constraining surface dynamics in data-limited settings on Earth (e.g. Durkin et al., 2017; Milliken et al., 2018) or other planets and moons (Goudge et al., 2018).

Backwater zones occur in the terminal reaches of rivers, where they meet a standing body of water in oceans or lakes (Chow, 1959). The length of the backwater zone (L_b) is estimated as $L_b \approx H/S$, where H is mean flow depth and S is the gradient of the water surface (Paola and Mohrig, 1996; Fig. 1). At the backwater transition, gravity-driven, normal flow conditions give way to temporally and spatially varying hydraulic conditions where both gravity and pressure gradients are important (Lane, 1957). As indicated by a number of recent studies, backwater hydrodynamics can influence sediment transport dynamics, the morphodynamics of rivers and floodplains, the position of delta avulsion nodes, as well as depositional trends over millennial to million-year timescales (Jerolmack and Swenson, 2007; Petter, 2010; Nittrouer et al., 2011a, 2011b, 2012; Lamb et al., 2012; Smith, 2012; Chatanantavet et al., 2012; Blum et al., 2013; Ganti et al., 2014, 2016; Fernandes et al., 2016; Mason and Mohrig, 2018; Trower et al., 2018; Martin et al., 2018).

The transition from normal flow to backwater-influenced flow (Fig. 1) in the Lower Mississippi River (LMR) occurs at approximately 600-750 river kilometers (RK; H=10-30 m, $S=10^{-5}$; Nittrouer et al., 2012). Studies of flow and sediment transport through the LMR reveal that flow decelerates downstream during low or moderate discharge ($<3x10^4$ m^3/s) and the terminal segment of the LMR acts as a "settling basin", accumulating a thick mantle of mud over channel bed and side-walls (Nittrouer et al., 2011a, 2012; Fig. 1). At high discharge ($>3x10^4$ m^3/s), the water level rises in the normal flow reach but remains relatively fixed near the river mouth, causing a downstream acceleration of flow and associated increase in bed material flux by two orders of magnitude across the lower RK200 (Nittrouer et al., 2012). During high-discharge events, easily suspended particles <0.3 mm in diameter sand are transported through the backwater zone and similarly partitioned between bedload and suspended load (Nittrouer et al., 2012), whereas >0.4 mm sand particles are thought to be transported as relatively slow-moving bedload within the

53 upper backwater zone (Wright and Parker, 2005; Nittrouer, 2013).These observations of sand-transport
54 through the lower MR lead to the inference that bar construction is primarily associated with high discharge
55 events, as this is the only time sand moves through the backwater zone. Here we test the hypothesis that
56 spatio-temporal variability in flow and sediment transport result in consistent spatial patterns in bank-
57 attached bar geometries, kinematics and sedimentology in the backwater zones of coastal rivers.

58 **The Balance of Forces Controlling the Transverse Slopes of Bars Constructed by Traction Load**

59 The transverse slope of a bar across which active bedload transport occurs is set by a balance of
60 forces: (1) the gravitational pull on the particle, acting in the downslope direction, and (2) the force acting
61 up the bar, induced by cross-stream circulation in bends (Dietrich and Smith, 1984; Sekine and Parker,
62 1992). The force F_d acting on individual sediment grains with diameter D as they are transported
63 downstream across the transverse bar slope θ can be expressed as:

64

65 $$F_d = \rho' g \, \pi \frac{1}{4} D^2 \ \ sin\theta \quad (1)$$

66

67 Where ρ' is the submerged density of silica sand in water and g is gravitational acceleration. This may also
68 be expressed as:

69

70 $$F_d \ \alpha \ \ D^2 \, sin\theta \quad (2)$$

71

72 When a resisting force exerted by the component of helical flow acting up the sloping bar surface balances
73 the effect of gravity, saltating sediment particles will move downstream across the transverse slope instead
74 of towards the thalweg (Dietrich and Smith, 1984; Sekine and Parker, 1992). This force is related to flow
75 velocity and the radius of curvature of the bend (Komar, 1969) as in:

76 $$F_r \ \alpha \ \rho \ \frac{u^2}{R_c} \quad (3)$$

Where R_c is the radius of curvature of the channel, ρ is the density of the fluid and u is the depth-averaged flow velocity.

When the forces are balanced,

$$sin\theta \; \alpha \; \frac{u^2}{D^2 R_c} \tag{4}$$

Therefore, for bends of a given curvature, cross-channel bar slope varies in proportion to (1) the square of the characteristic velocity associated sediment transport at high discharge through bends in the backwater zone and (2) the inverse of the representative particle size in traction load squared. Thus, if the depth-averaged flow velocity increases (Nittrouer et al., 2012) downstream across the backwater zone and particle sizes available for bar construction decrease, this relationship predicts a downstream increase in the transverse slopes of bars.

Bank-attached Bar Composition and Geometry across the Backwater Zone of the Mississippi River

We present spatial patterns in geometry and composition using data from 1265 borehole logs compiled by the U.S. Army Corps of Engineers (USACE) in the Late Holocene Mississippi channel belt (MCB; Fig. 1b) (Saucier, 1994; Fernandes et al., 2016), grain-size data of bed material from the modern MR (U. S. Army Corps of Engineers, 1935) and bathymetry collected in 1913 (See Data Repository (DR)). All these data sources pre-date significant engineering modification to the MR channel, though we acknowledge that some anthropogenic impact may manifest even in these data. Sedimentary facies from boreholes, which represent millennial-scale sedimentation patterns, were used to characterize bulk facies changes across the backwater zone. We used: (A) mud- rich residual channel fills as proxies for MCB thickness (Fernandes et al., 2016), (B) sand and mud deposited at the tops of point bars as proxies for easily-suspended sediment load, and (C) a mix of sand and gravel beneath Facies B, interpreted as the undifferentiated deposits of bedload-dominated MCB point bars and underlying Pleistocene braided rivers. Downstream of RK400, where oxbow lakes are absent, the thickness of Facies B was used as a proxy for

MCB thickness (Fernandes et al., 2016); between RK300-RK400, only thicknesses that exceeded the p75 of Facies B were used. A comparison of the two sets of measurements provided a proxy for the contribution of easily suspended material to MCB bars, from just downstream of Cairo, Illinois (RK1250) to Head of Passes (RK0) (Fig. 2A). Downstream of RK500, the MCB thickens and bars incorporate increasing amounts of Facies B, which dominates channel-belt deposits between RK0 and RK200. The bed material load (Fig. 2B) grows enriched in particle sizes <0.3 mm (medium grained sand) downstream of RK200, the likely result of long-term storage of "perennial" bedload (>0.4 mm) in the upper backwater zone (U. S. Army Corps of Engineers, 1935). Notably, the limit of the slow-moving gravel front occurs in the vicinity of RK400, near Baton Rouge (Nittrouer, 2013, Fig. 2B).

We measured the cross-channel slopes of bank-attached bars (Fig. 2C, E, F) as well as the planform shape of the bar surfaces using the bathymetric data from RK500 to RK0. The percentiles (p) of measurements within a RK100 show increases (Fig. 2C, E) from upstream of RK400 (p10=1^{o}, p25=2^{o}, p50=3^{o}, p75=4^{o}; p90=5^{o}) to downstream of RK300 (p10=2.5^{o}, p25=3^{o}, p50=4^{o}, p75=4.5^{o}-5.5^{o}; p90=6^{o}-7.5^{o}); distributions also become increasingly skewed towards higher slopes downstream of RK350. Suspension-dominated sediment deposition, in flow-separation zones downstream of high curvature bends or point bars, can display very high slopes (Smith et al., 2009). We evaluated the curvature of bars in context of the transverse slopes (Fig. 2D). Curvatures of bar deposits, expressed as the inverse of radii of curvature and assigned different signs depending on whether they were convex or concave with respect to the channel centerline (Fig. 2F), do not show any systematic spatial trend in the relative abundance of these shapes. Steepness of both convex and concave portions of bars increase downstream. Therefore, the backwater dynamics do appear to cause a systematic increase in transverse bar slopes; the distributions of planform curvatures of bars, however, appear unaffected within the studied reach.

Linking the Kinematics and Geometry of Bars across the Backwater Zone of the Mississippi and Trinity Rivers

In the past, authors have hypothesized that downstream changes in channel lateral migration rates are linked to spatially variable sediment storage in bars and cross-stream bar geometry (Ikeda, 1989; Smith,

2012; Nittrouer et al., 2012; Blum et al., 2013; Fernandes et al., 2016). We test this idea by comparing the transverse bar slopes and lateral migration rates (Fig.3) of two alluvial rivers: 1) the Lower Trinity River (LTR), Texas, (Smith, 2012; Smith and Mohrig, 2017; Mason and Mohrig, 2018; Smith et al., in review), 2) the LMR (Hudson and Kesel, 2000). The LTR is a sand-bedded river with an insignificant amount of engineered modification in the studied region. Sediment samples from bars across the backwater zone reveal uniform distributions of sand-sized (<1.5 mm) sediment; however, gravel-sized particles, observed in samples from near the backwater transition, are absent from the samples in the lower backwater zone (Smith, 2012; Smith et al., in review). Both rivers have bathymetry collected over the required river channel length to compute the cross-channel slopes of bars and sufficient time-lapse information to compute lateral channel migration rates respectively.

To account for their very different scales, we divided distances upstream of the terminus of the LMR and LTR by the respective backwater lengths of each river and lateral migration rates by the mean channel width (Table 1, Fig.3). Transverse slopes of bars in both rivers follow similar trends; they show a systematic and similar increase downstream of the backwater transition in both rivers (Fig. 3). This is likely to be in response to downstream fining of bed material (Smith, 2012; Smith et al., in review) and/or downstream acceleration at high discharge. Channel migration rates for both rivers increase at the normal flow to backwater transition (dimensionless distance = 1) but decrease drastically downstream across the backwater zone (Fig. 2). This is probably a consequence of sand storage at the backwater transition (Nittrouer et al., 2012; Smith, 2016; Fernandes et al., 2016). Channel asymmetry in normal flow, associated with prolific bar growth and shallower cross-channel slopes at the backwater transition, likely contributes to topographic steering of high-velocity flow, enhanced erosion of the outer bank and locally accelerated lateral migration (Ikeda et al., 1981; Eke et al., 2014).

Discussion

The systematic and predictable increase in the cross-stream slopes of the two studied rivers and reduction in particle size of sediment, coupled with a reduction in the lateral migration rates downstream of the backwater transition zone, indicate that the dynamics of flow and sediment transport across the

backwater zone have a fundamental impact on the kinematics, composition and geometry of bank-attached bars (Ikeda, 1989; Smith, 2012; Nittrouer et al., 2012; Fernandes et al., 2016). Furthermore, the proposed force balance scaling likely represents a sound first step towards explaining observed trends in cross-channel bar slopes through the backwater zone. Figures 2 A, B and C offer the intriguing opportunity for connecting (1) the spatio-temporal non-uniformity in sediment-transport dynamics, to (2) the spatial variability of sedimentary facies, in terms of relative sand and mud content, and (3) the dip of preserved bar accretion sets in the sedimentary record of fluvial backwater zones. This is particularly relevant to paleo-environmental reconstructions in data-limited settings. At the scale of rock outcrops, the sedimentary record of laterally mobile channels is dominated by inclined bed-sets formed through bar accretion (Colombera et al., 2017; Durkin et al., 2017; Mahon and McElroy, 2018). Statistically robust spatial trends in the steepness of dipping bar surfaces and the relative proportions of sand and mud in coastal channel belts may serve to locate outcrops along proximal-to-distal paleo-river profiles. The distribution of slopes in the preserved remnants of bar surfaces, however, may be somewhat different from that observed in modern channels. To our knowledge, a formal statistical treatment of this preservation bias has not yet been attempted and may be needed to further quantify uncertainties associated with these trends in the sedimentary record.

The current work adds to a growing body of research in which a unifying hydraulic framework is used to elucidate the expected spatial variability in (1) the large-scale geometry of channel belts (i.e. thickness and width), (2) the sedimentary facies, (3) the expected scales of channel bed scours, and (4) geometry of bar deposits filling channel belts, in backwater-influenced paleo-channels (Petter, 2010; Blum et al., 2013; Fernandes et al., 2016; Trower et al., 2018; Martin et al., 2018). These attributes, applicable at different scales of investigation (e.g. remotely sensed channel belts, outcrops or sediment cores), can be used to reconstruct past environments and dynamics of fluvio-deltaic systems on Earth or other planetary bodies and to predict sub-surface heterogeneity and reservoir potential.

Conclusions

Our comparison of trends in the Lower Mississippi and Lower Trinity Rivers suggests that backwater hydrodynamics and sediment transport dynamics constitute fundamental controls on the sedimentology, geometry and kinematics of bars observed in these systems. These results therefore define a critical link between backwater dynamics and bed-scale stratal geometries, providing a process-based framework for reconstructing paleo-dynamics and -environment from ancient sedimentary strata on Earth and other planets and for predicting reservoir-scale attributes in remotely sensed settings.

Acknowledgements

The authors would like to acknowledge the efforts of the many scientists working for the Trinity River Authority, Texas Parks and Wildlife and the U.S. Army Corps of Engineers who collected much of the data used in this paper.

References Cited

Blum, M., Martin, J., Milliken, K., and Garvin, M., 2013, Paleovalley systems: insights from Quaternary analogs and experiments: Earth-Science Reviews, v.116, p. 128 – 169.

Chatanantavet, P., Lamb, M.P., and Nittrouer, J.A., 2012, Backwater controls of avulsion location on deltas: Geophysical research letters, v. 39, p. L01402, doi: 10.1029/2011GL050197.

Colombera, L., Mountney, N.P., Russell, C.E., Shiers, M.N., and McCaffrey, W.D., 2017, Geometry and compartmentalization of fluvial meander-belt reservoirs at the bar-form scale: Quantitative insight from outcrop, modern and subsurface analogues: Marine and Petroleum Geology, v. 82, p. 35–55, doi:10.1016/j.marpetgeo.2017.01.024.

Dietrich, W.E., and Smith, J.D., 1984, Bed Load Transport in a River Meander: Water resources research, v. 20, p. 1355–1380, doi:10.1029/WR020i010p01355.

Durkin, P.R., Boyd, R.L., and Hubbard, S.M., 2017, Three-dimensional reconstruction of meander-belt evolution, Cretaceous McMurray formation, Alberta Foreland Basin, Canada: Journal of Sedimentary Research, v.87, p.1075-1099, doi: 10.2110/jsr.2017.59

Eke, E., Parker, G., and Shimizu, Y., 2014, Numerical modeling of erosional and depositional bank processes in migrating river bends with self-formed width: Morphodynamics of bar push and bank pull: Journal of Geophysical Research: Earth Surface, v. 119, p. 1455–1483,

doi:10.1002/2013JF003020

Fernandes, A.M., Törnqvist, T.E., and Straub, K.M., 2016, Connecting the backwater hydraulics of coastal rivers to fluvio-deltaic sedimentology and stratigraphy, v. 44, p. 979–982, doi: 10.1130/G37965.1

Ganti, V., Chadwick, A.J., Hassenruck-Gudipati, H.J., Fuller, B.M., and Lamb, M.P., 2016, Experimental river delta size set by multiple floods and backwater hydrodynamics: Science advances, v. 2, p. e1501768, doi:10.1126/sciadv.1501768.

Ganti, V., Chu, Z., Lamb, M.P., Nittrouer, J.A., and Parker, G., 2014, Testing morphodynamic controls on the location and frequency of river avulsions on fans versus deltas: Huanghe (Yellow River), China: Geophysical research letters, v. 41, p. 2014GL061918, doi:10.1002/2014GL061918.

Goudge, T.A., Mohrig, D., Cardenas, B.T., Hughes, C.M., and Fassett, C.I., 2018, Stratigraphy and paleohydrology of delta channel deposits, Jezero crater, Mars: Icarus, v. 301, p. 58–75, doi:10.1016/j.icarus.2017.09.034.

Hudson, P.F., and Kesel, R.H., 2000, Channel migration and meander-bend curvature in the lower Mississippi River prior to major human modification: Geology, v. 28, p. 531–534, doi:2.0.CO;2">10.1130/0091-7613(2000)28<531:CMAMCI>2.0.CO;2.

Ikeda, H., 1989, Channel Migration and Point bar origin in sandy meanders, *in* Ikeda, S. and Parker, G. eds., River Meandering, American Geophysical Union, p. 51–68.

Ikeda, S., Parker, G., and Sawai, K., 1981, Bend theory of river meanders. Part 1. Linear development: Journal of Fluid Mechanics, v.112, p. 363-377.

Jerolmack, D.J., and Swenson, J.B., 2007, Scaling relationships and evolution of distributary networks on wave-influenced deltas: Geophysical Research Letters, v. 34, doi:10.1029/2007GL031823.

Kolker, A.S., Cable, J.E., Johannesson, K.H., and Allison, M.A., 2013, Pathways and processes associated with the transport of groundwater in deltaic systems: Journal of Hydrology, v. 498, p. 319-334, doi: 10.1016/j.jhydrol.2013.06.014

Komar, P.D., 1969, The channelized flow of turbidity currents with application to Monterey Deep-Sea Fan Channel: Journal of geophysical research, v. 74, p. 4544–4558, doi:10.1029/JC074i018p04544.

Lamb, M.P., Nittrouer, J.A., Mohrig, D., and Shaw, J., 2012, Backwater and river plume controls on

scour upstream of river mouths: Implications for fluvio-deltaic morphodynamics: Journal of Geophysical Research: Earth Surface, v. 117, F01002, doi:10.1029/2011JF002079.

Lane, E. W., 1957, A Study of the Shape of Channels Formed by Natural Streams Flowing in Erodible Material, U.S. Army Corps of Engineers, Mo. River Div., Omaha, Nebr.

Mahon, R.C., and McElroy, B., 2018, Indirect estimation of bedload flux from modern sand-bed rivers and ancient fluvial strata: Geology, v. 46, p. 579–582. doi:10.1130/G40161.1.

Martin, J., Fernandes, A.M., Pickering, J., Howes, N., Mann, S., and McNeil, K., 2018, The Stratigraphically Preserved Signature of Persistent Backwater Dynamics in a Large Paleodelta System: The Mungaroo Formation, North West Shelf, Australia: Journal of Sedimentary Research, v. 88, p. 850–872, doi:10.2110/jsr.2018.38.

Mason, J., and Mohrig, D., 2018, Using time-lapse lidar to quantify river bend evolution on the meandering coastal Trinity River, Texas, USA: Journal of Geophysical Research: Earth Surface, v. 123, 1133–1144. Doi:10.1029/ 2017JF004492

Milliken, K.T., Blum, M.D., Snedden, J.W., and Galloway, W.E. Application of fluvial scaling relationships to reconstruct drainage-basin evolution and sediment routing for the Cretaceous and Paleocene of the Gulf of Mexico: Geosphere, v. 14, p. 1–19, doi:10.1130/GES01374.1.doi:10.1130/GES01374.1.

Nittrouer, J.A., 2013, Backwater hydrodynamics and sediment transport in the lowermost Mississippi River Delta: Implications for the development of fluvial-deltaic landforms in a large lowland river: Deltas: Landforms, Ecosystems, and Human Activities: International Association of Hydrological Sciences Publication, v. 358, p. 48–61.

Nittrouer, J.A., Mohrig, D., and Allison, M., 2011a, Punctuated sand transport in the lowermost Mississippi River: Journal of Geophysical Research, v. 116, p. F04025, doi:10.1029/2011JF002026.

Nittrouer, J.A., Mohrig, D., Allison, M.A., and Peyret, A.-P.B., 2011b, The lowermost Mississippi River: a mixed bedrock-alluvial channel: Sedimentology, v. 58, p. 1914–1934, doi:10.1111/j.1365-3091.2011.01245.x.

Nittrouer, J.A., Shaw, J., Lamb, M.P., and Mohrig, D., 2012, Spatial and temporal trends for water-flow velocity and bed-material sediment transport in the lower Mississippi River: GSA Bulletin, v. 124, p. 400–414, doi:10.1130/B30497.1.

Paola, C., and Mohrig, D., 1996, Palaeohydraulics revisited: palaeoslope estimation in coarse-grained braided rivers: Basin Research, v. 8, p. 243–254, doi:10.1046/j.1365-2117.1996.00253.x.

Petter, A.L., 2010, Stratigraphic implications of the spatial and temporal variability in sediment transport in rivers, deltas, and shelf margins [Ph.D. thesis]: Austin, University of Texas at Austin, 205 p.

Saucier, R.T., 1994, Geomorphology and Quarternary Geologic History of the Lower Mississippi Valley. Volume 2: AU. S. Army Corps of Engineers, Waterways Experiment Station.

Sawyer, A.H., Edmonds, D.A., and Knights, D., 2015, Surface water-groundwater connectivity in deltaic distributary channel networks: Geophysical Research Letters, v. 42, p. 10,299–10,306, doi:10.1002/2015GL066156.

Sekine, M., and Parker, G., 1992, Bed-load transport on transverse slope. I: Journal of Hydraulic Engineering, v. 118, p. 513–535, doi:10.1061/(ASCE)0733-9429(1992)118:4(513).

Smith, V.B., 2012, Geomorphology of a coastal sand-bed river: Lower Trinity River, Texas [Ph.D. thesis]: Austin, University of Texas at Austin

Smith, D.G., Hubbard, S.M., Leckie, D.A., and Fustic, M., 2009, Counter point bar deposits: lithofacies and reservoir significance in the meandering modern Peace River and ancient McMurray Formation, Alberta, Canada: Sedimentology, v. 56, p. 1655–1669, doi:10.1111/j.1365-3091.2009.01050.x.

Smith, V.B., and Mohrig, D., 2017, Geomorphic signature of a dammed Sandy River: The lower Trinity River downstream of Livingston Dam in Texas, USA: Geomorphology, v.297, p. 122-136.

Smith, V.B., Mason, J., and Mohrig, D., Morphodynamics of a Backwater Influenced Sand-bed River: The Lower Trinity River, Texas, USA, *in review*, Earth and Planetary Science Letters.

Chow, V. T., 1959, Open-channel hydraulics: McGraw-Hill New York, v. 1.

Trower, E.J., Ganti, V., Fischer, W.W., and Lamb, M.P., 2018, Erosional surfaces in the Upper Cretaceous Castlegate Sandstone (Utah, USA): Sequence boundaries or autogenic scour from backwater hydrodynamics? Geology, v. 46, p. 707-710. doi:10.1130/G40273.1.

U. S. Army Corps of Engineers, 1935, Studies of River Bed Materials and their Movement, with Special Reference to the Lower Mississippi River: U. S. Army Corps of engineers, Waterways Experiment Station Paper 17.

Wright, S., and Parker, G., 2005, Modeling downstream fining in sand-bed rivers. I: formulation: Journal of Hydraulic Research, v. 43, p. 613–620, doi:10.1080/00221680509500381.

Figures Captions

Figure 1: Schematic summary of spatial and temporal patterns in water surface slope, predicted sediment transport trends (from Nittrouer et al., 2012) and terminology used.

Figure 2: (A) Thickness of the channel belt and of Facies B from RK1200 to RK0. The 10th, 25th, 50th, 75th, 90th (p10, p25, p50, p75, p90) percentiles were calculated using a moving window equal to 100RK. (B) Grain-size trends from bed material samples shown as the D50 (50th percentile of all nominal diameters) of the bed sample as well as the mean p10, p25, p50, p75, and p90 of all samples collected within a 50RK window of the sample location. (C) Cross-stream slopes of bank-attached bars in degrees, as well as the p10, p25, p50, p75, and p90 of all measurements within a moving100RK window. (D) Planform curvature of bars, expressed as convexity (positive values) and concavity (negative values). The median of all convex and concave curvatures in moving 100RK windows is given by the solid black line; the p25, p50, p75 of convex and concave shapes in 100RK windows are given by the red and grey envelopes respectively. Colored crosses show the measured cross stream slopes for all curvatures. (E) Spatial pattern in transverse slopes of bars. Insets (F and G) show details of the Late Holocene bar deposits (grey polygon), their centroids (red crosses), channel banks (black dotted lines) and channel centerline (blue dotted lines). (F) Detail of planform geometry at different points along the channel bank (G) Detail of measured mean slopes of the cross-stream bar surfaces.

Figure 3: Comparison of (A) cross-stream bar slopes and (B) lateral migration rates observed in the Lower Mississippi and Trinity Rivers. Distance upstream of the river mouth is standardized by the backwater length in both plots, and lateral migration rates in (B) are standardized by the mean channel width.

313

314 Table 1: Attributes used to scale the Mississippi and Trinity Rivers in Figure 3.

	Backwater Length (km)	Mean Channel Width (m) in the backwater zone
Lower Trinity River, Texas, U. S. A.	50	70
Lower Mississippi River, U. S. A.	700	900

315

316

317 Figure 1

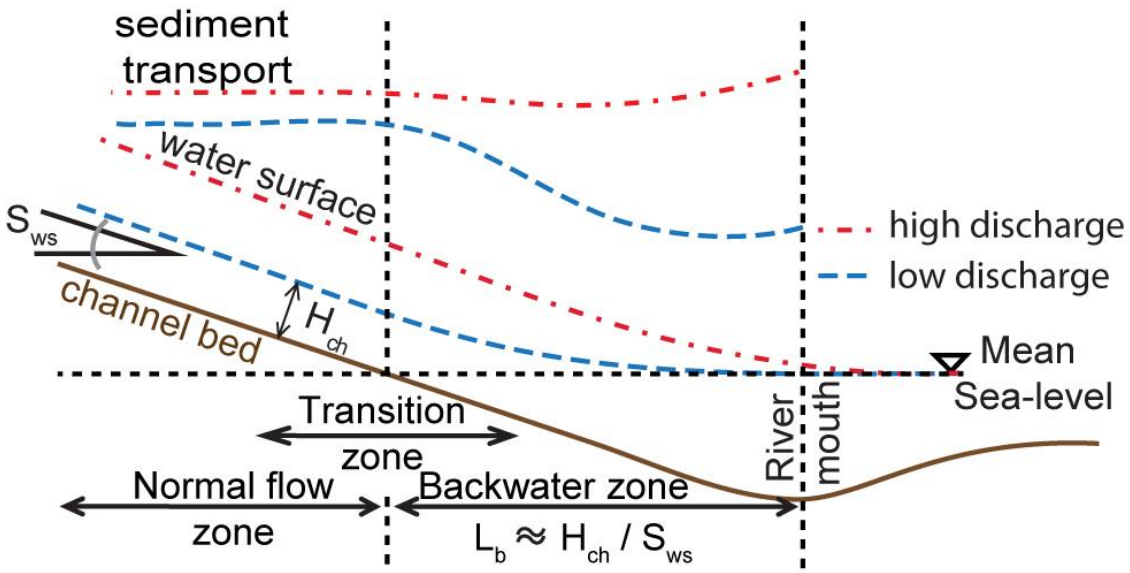

318

319

Figure 2

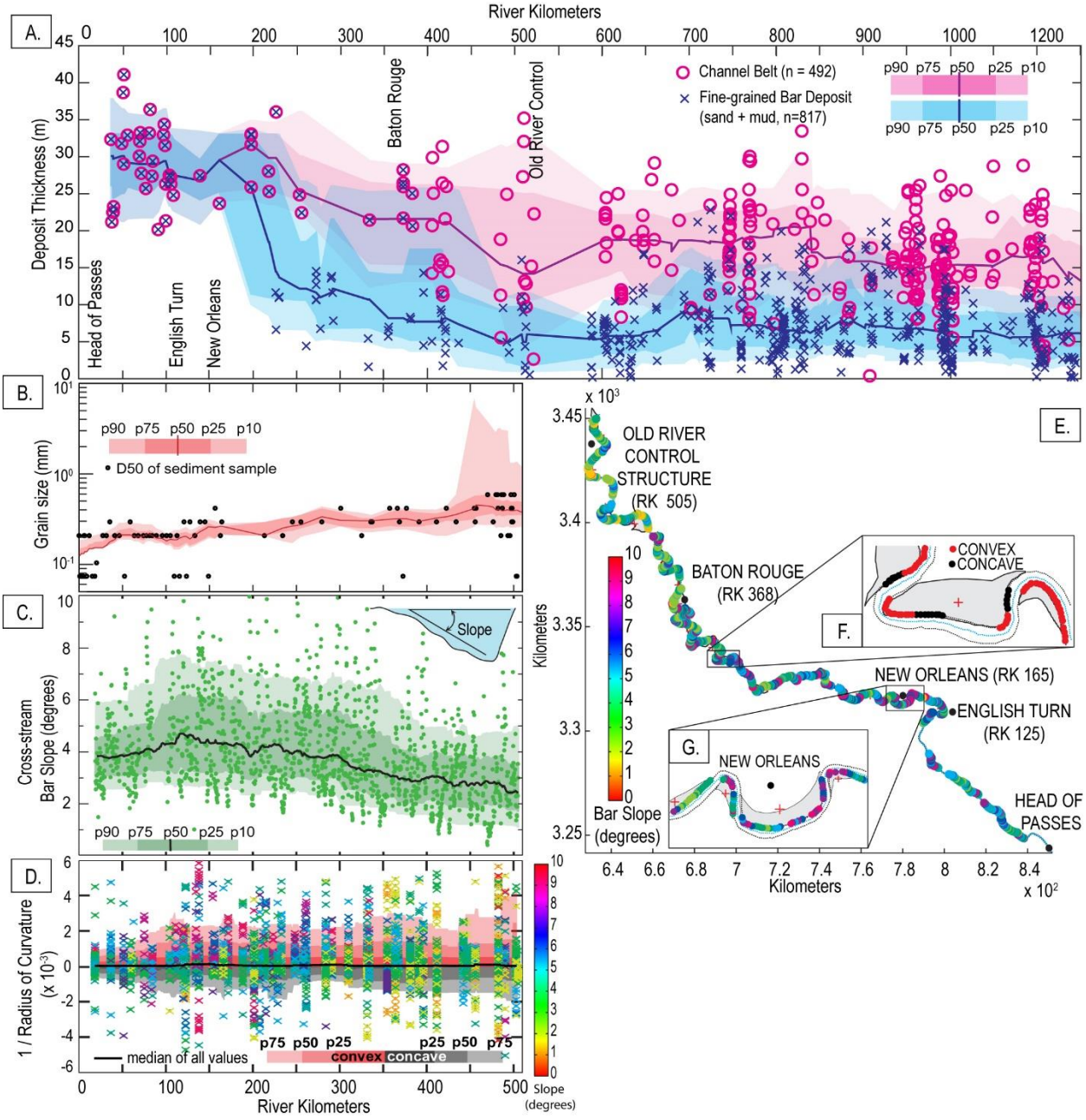
A.
River Kilometers
Deposit Thickness (m)
Channel Belt (n = 492)
Fine-grained Bar Deposit
(sand + mud, n=817)
p90 p75 p50 p25 p10
Baton Rouge
Old River Control
Head of Passes
English Turn
New Orleans
B.
Grain size (mm)
D50 of sediment sample
C.
Cross-stream
Bar Slope (degrees)
Slope
D.
1 / Radius of Curvature
(x 10⁻³)
median of all values
convex
concave
River Kilometers
Slope
(degrees)
E.
OLD RIVER
CONTROL
STRUCTURE
(RK 505)
BATON ROUGE
(RK 368)
NEW ORLEANS (RK 165)
ENGLISH TURN
(RK 125)
HEAD OF
PASSES
Kilometers
Bar Slope
(degrees)
F.
CONVEX
CONCAVE
G.
NEW ORLEANS

328 Figure 3

329

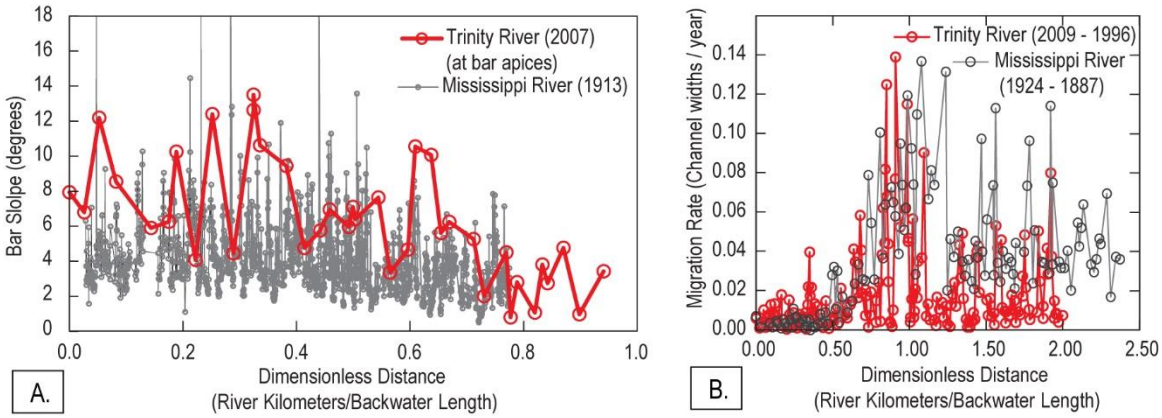

330